

Preparation of a main-chain azo polyurethane-urea and its application of Y-branch and Mach–Zehnder thermo-optic switch

Zhijuan Cao · Fengxian Qiu · Guorong Cao ·
Yijun Guan · Lin Zhuang · Feiyan Ye · Dongya Yang

Received: 11 September 2012 / Accepted: 18 November 2014 / Published online: 26 November 2014
© Springer-Verlag Berlin Heidelberg 2014

Abstract A novel main-chain azo polyurethane-urea (MCAPUU) was prepared with chromophore molecule 1,1'-azobisformamide (ABFA), polyether polyol (NJ-220) and isophorone diisocyanate (IPDI). The chemical structures of ABFA monomer and MCAPUU were characterized by the FT-IR and UV–Visible spectroscopy. The thermal and mechanical properties of MCAPUU film were investigated. The refractive index and transmission loss of MCAPUU film were measured at different temperature and different laser wavelength by attenuated total reflection (ATR) technique and the CCD digital imaging devices. The thermo-optic coefficients (dn/dT) of MCAPUU are $-4.5429 \times 10^{-4} \text{ } ^\circ\text{C}^{-1}$ (532 nm), $-5.7943 \times 10^{-4} \text{ } ^\circ\text{C}^{-1}$ (650 nm) and $-6.6057 \times 10^{-4} \text{ } ^\circ\text{C}^{-1}$ (850 nm), respectively. A Y-branch switch and Mach–Zehnder interferometer (MZI) thermo-optic switches based on thermo-optic effect were proposed and the performances of switches were simulated. The results showed that the power consumption of the Y-branch thermo-optic switch is only 0.74 mW. The rising and falling times of Y-branch and MZI switches are 12.0 and 1.8 ms, respectively. The results indicate that the prepared MCAPUU has high potential for the applications of the Y-branch digital optical switch (DOS), MZI thermo-optic switch, directional coupler (DC) switch and optical modulators.

Electronic supplementary material The online version of this article (doi:[10.1007/s00289-014-1275-2](https://doi.org/10.1007/s00289-014-1275-2)) contains supplementary material, which is available to authorized users.

Z. Cao · F. Qiu (✉) · F. Ye · D. Yang
School of Chemistry and Chemical Engineering, Jiangsu University,
Zhenjiang 212013, China
e-mail: fxqiu@chem@163.com

G. Cao · Y. Guan · L. Zhuang
Department of Physics, Jiangsu University, Zhenjiang 212013, China

Keywords Polyurethane-urea · Thermo-optic coefficient · Thermo-optic switch · Mach–Zehnder interferometer (MZI) switch

Introduction

In recent years, polymeric materials containing azo chromophore have gained a great deal of attention due to their unique optical property. These azo polymers can be potentially applied in fascinating photo-responsive variations, such as liquid crystal displays [1], optical information data storage [2, 3], optical switching [4, 5], nonlinear optical materials [6, 7], holographic surface relief gratings (SRGs) [8], holographic memories [9, 10] and so on. The azo chromophore can be incorporated into polymers and become side chains [11, 12] or parts of the polymer main chains [13] via chemical reaction. Compared with the side-chain polymer, main-chain azo polymers showed good thermal stability (high glass-transition temperature (T_g) and thermal decomposition temperature (T_d) [14]).

Optical switches and related arrays play an important role in optical communication networks. Compared to the micro-optoelectronic mechanical switches and liquid-crystal switches, the waveguide switches show wide potential application for their high reliability. Waveguide optical devices [15–17] have attracted a lot of research interest recently, not only because of their small device sizes, but also because of the possibility of achieving reconfigurable functionality as well as large scale integration. Among various optical waveguide devices that have been studied, the thermo-optic waveguide switch is one of the fundamental device structures that are essential for achieving reconfigurable functionality through their optical switching function. The thermo-optic effect within polymer optical waveguides is useful for realizing integrated optic components with optical switching and tuning capability. Various polymeric thermo-optic switches have been reported including digital optical switches (DOS), Mach–Zehnder interferometer switches, directional coupler switches, multimode interference/vertical coupler switches and thermo-optic total-internal-reflection switches [18–20]. These devices show great promise in low-speed fiber-optic communication systems and have been successively implemented in commercially integrated devices.

Yulianti et al. [21] reported a digital optical switch (DOS) with different branching angle and short device length based on UV curable fluorinated resin. The thermo-optic coefficient (TOC) and thermal conductivity of material were $-1.7 \times 10^{-4} \text{ }^\circ\text{C}^{-1}$ and 0.17 W/(mK) , respectively. The Y-branch shape was optimized by introducing constant effective refractive index difference between branches along the propagation direction through beam propagation method (BPM) scheme. With branching angle of 0.299° and device length of only 5 mm, the simulation result showed that the device could exhibit crosstalk of -33 dB at calculated required power of only 26 mW. Cao et al. [22] proposed a Mach–Zehnder interferometer thermo-optic switch based on DR1/PMMA. The total length of the device is 3.5 cm including the 1.5-cm heater. The extinction ratio, the power consumption and switching time are 21 dB, 13 mW and 0.9 ms, respectively. Lee

et al. [23] reported a fully packaged polymeric four arrayed 2×2 digital optical switch with crosslinkable fluorinated polymers. The crosstalks were less than -30 dB for all four 2×2 digital optical switch elements with each total electrical power of 250 mW. The fall and rise times were less than 5 ms. In this paper, a Y-branch and Mach–Zehnder interferometer (MZI) switch with two rib waveguides, dual driving electrodes and two critical 3-dB couplers polymeric thermo-optic switches based on thermo-optic effect of prepared MCAPUU were designed and simulation. This work exhibits thermo-optic device based on novel main-chain azo polymer. To the best our knowledge, this is the first time that the prepared main-chain azo polyurethane-urea (MCAPUU) is reported.

Experimental

Materials

1,1'-Azobisformamide (ABFA), *N,N*-dimethylformamide (DMF) and dibutylbis (lauroxy) tin (T-12) were supplied from Sinopharm Chemical Reagent Co., Ltd. in Shanghai, China. Polyether polyols (NJ-220, $M_n = 2,000$ g/mol) was produced by Ningwu Chemical CO., Ltd. in Jurong, Jiangsu, China. Isophorone diisocyanate (IPDI) was supplied by Rongrong Chemical Co., Ltd. in Shanghai, China.

Characterizations and performance measurements

Structure characterization

FT-IR spectra of samples were recorded between $4,000$ and 400 cm^{-1} on a KBr pellet with an FTIR spectrometer (AVATAR 360, Madison, Nicolet). A minimum of 32 scans was signal-averaged with a resolution of 2 cm^{-1} in the $4,000$ – 500 cm^{-1} ranges. Ultraviolet–visible (UV–Vis) spectra of samples were recorded with a Shimadzu (Japan) UV-2450 spectrometer at 25 °C. The contents of ABFA and prepared MCAPUU were 3.0 mg/L.

Thermal property

Differential scanning calorimetry (DSC) and thermogravimetric analysis (TGA) were performed on a Netzsch (Germany) STA 449C instrument. The programmed heating range was from room temperature to $1,000$ °C at a heating rate of 10 °C/min under a nitrogen atmosphere. The measurement was taken with 6 – 10 mg samples.

Mechanical property

The tensile strength and elongation at break testing for polymer film were carried out on a tensile tester (KY-8000A, Jiangdu Kaiyuan Test Machine, Jiangdu, China) at room temperature at a speed of 50 mm min^{-1} . All measurements had an average of three runs. The dumbbell-type specimen was of 30 mm length at two ends,

0.2 mm thick and 4 mm wide at the neck. The hardness was measured with a sclerometer (KYLX-A, Jiangdu Kaiyuan Test Machine) (Jiangdu, China); measurements were done three times for the polymer sample, and the average value was calculated.

Physical property

The thermal conductivity, thermal diffusion coefficient and specific heat capacity of polymer film were obtained from a thermal conductivity detector (TC3010, Xi'an Xiayi Electronic Technology Co., Ltd, Xi'an, China) at room temperature.

Measurement of refractive index of MCAPUU film

Measurement of refractive index was performed using attenuated total reflection (ATR) technique. The dielectric planar waveguide is a three-tier. The waveguide layer is between the substrate and cover layer. The refractive indices of substrate-based, guided-wave layer and cover layer are assumed to be n_2 , n_1 and n_0 , respectively. The guided-wave thickness is assumed to be h . For the TM polarization mode, dispersion equation can be expressed as follows:

$$\kappa h = m\pi + \tan^{-1}\left(\frac{n_1^2 p}{n_2^2 \kappa}\right) + \tan^{-1}\left(\frac{n_1^2 q}{n_0^2 \kappa}\right) \quad (1)$$

There is

$$\kappa = (k_0^2 n_1^2 - \beta^2)^{1/2}, \quad p = (\beta^2 - k_0^2 n_2^2)^{1/2}, \quad q = (\beta^2 - k_0^2 n_0^2)^{1/2}$$

where $k_0 = 2\pi/\lambda$ is the wave vector (vacuum), λ is the wavelength of the laser and m is mode order number. β is the propagation constant for guided-mode, K is the wave vector of the z -component, κ is the x -component of the wave vector K , $K = k_0 n_1$.

The effective refractive index of guided mode is defined $N = \beta/k_0$. The effective refractive index can be calculated by measuring the angle of sample and the guided-mode propagation constant β was also obtained.

For multi-mode waveguide, if propagation constants (β_{m-1} , β_m and β_{m+1}) of the three modes are obtained, the transcendental equations can be expressed:

$$\begin{aligned} \kappa_{m-1} h &= (m-1)\pi + \tan^{-1}\left(\frac{n_1^2 p_{m-1}}{n_2^2 \kappa_{m-1}}\right) + \tan^{-1}\left(\frac{n_1^2 q_{m-1}}{n_0^2 \kappa_{m-1}}\right) \\ \kappa_m h &= m\pi + \tan^{-1}\left(\frac{n_1^2 p_m}{n_2^2 \kappa_m}\right) + \tan^{-1}\left(\frac{n_1^2 q_m}{n_0^2 \kappa_m}\right) \\ \kappa_{m+1} h &= (m+1)\pi + \tan^{-1}\left(\frac{n_1^2 p_{m+1}}{n_2^2 \kappa_{m+1}}\right) + \tan^{-1}\left(\frac{n_1^2 q_{m+1}}{n_0^2 \kappa_{m+1}}\right) \end{aligned} \quad (2)$$

From these equations, refractive index n_1 of MCAPUU at different temperature can be obtained.

Measurement of Transmission loss of MCAPUU film

Transmission loss of optical waveguide devices is produced mainly by the following factors: waveguide material loss caused by scattering and absorption; substrate surface finish by polishing process constraints, irregular interface leading coupling loss between guided mode and radiation mode; curved waveguide surface, causing the loss caused by energy radiation. The digital imaging device charge coupled device (CCD) was used to record the scattered light intensity of points on the transmission line and transfer it into an internal light intensity.

After spatial average filter, a transmission attenuation curve can be obtained. The attenuation loss of the guided mode power with propagation distance can be expressed as follows:

$$P_Z = P_0 e^{(-\alpha \cdot Z)}, \quad (3)$$

where P_0 is initial incident light intensity of $Z = 0$, P_Z is transmission light intensity of $Z = z$ and the attenuation coefficient is defined as:

$$\alpha = \frac{1}{z_2 - z_1} \ln \left(\frac{P_{z_1}}{P_{z_2}} \right) \quad (4)$$

$$L = -10\alpha(\lg e) \quad (5)$$

L is the transmission loss of optical waveguide.

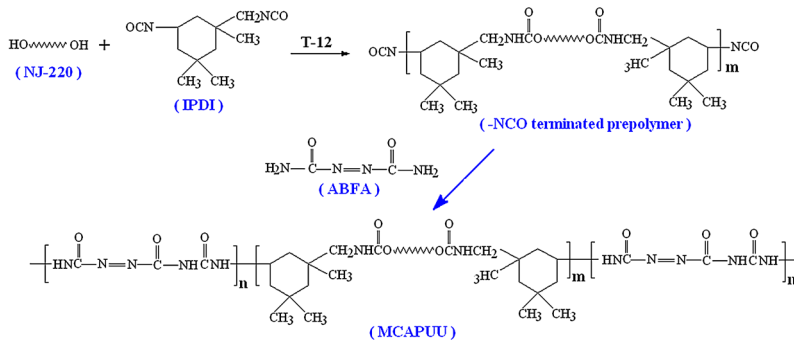
Preparation of main-chain azo polyurethane-urea (MCAPUU)

The polyether polyol (NJ-220, 20 g), IPDI (5.6 g) and DMF (15 mL) were added into a 250 mL three-neck round-bottom flask equipped with a mechanical stirrer, thermometer and reflux condenser. The dibutylbis (lauroxy)tin (T-12, 1.0 mL) as a catalyst was added to the solution and maintained at 80 °C for 3 h to prepare the –NCO terminated prepolymer. Then the chromophore molecule 1,1'-azobisformamide (ABFA, 2.4 g) dissolved in DMF (12 mL) was dropped into the mixture. The reactant refluxed for 3 h at 80 °C. The product was purified on a silica gel column with the eluate DMF. The synthetic route of main-chain azo polyurethane-urea (MCAPUU) is shown in Scheme 1.

Results and discussion

Structure characterization

The UV–Vis absorption spectra of ABFA monomer and the prepared main-chain azo polyurethane-urea MCAPUU are shown in Supplementary information Figure S1. It can be seen that the maximum absorption peaks of the ABFA and



Scheme 1 The synthetic route of main-chain azo polyurethane-urea (MCAPUU)

MCAPUU are observed at 270 and 251 nm, respectively. The peaks are mainly due to by the $\pi - \pi^*$ transitions of the absorption peak ($-\text{N}=\text{N}-$ groups).

The FT-IR spectra of the ABFA monomer and main-chain azo polyurethane-urea MCAPUU are shown in Supplementary information Figure S2. From the FT-IR spectrum of ABFA, the absorption band at $3,500\text{--}3,580\text{ cm}^{-1}$ is assigned to the stretching vibration of free and hydrogen-bonded $-\text{NH}$ groups. It can be seen the absorption peak of $2,928\text{ cm}^{-1}$ corresponds to the stretch vibration of $\text{Ar}-\text{H}$ bond. The band at $1,259\text{ cm}^{-1}$ is assigned to the stretch vibration of $\text{C}-\text{N}$ bond. A broad band at $1,680\text{ cm}^{-1}$ is assigned to the carbonyl of $-\text{NHCONH}-$ groups. The band located at $1,505\text{ cm}^{-1}$ is attributed to the symmetrical vibration of $-\text{N}=\text{N}-$ group, indicating that the $-\text{N}=\text{N}-$ group existed. From the FT-IR spectrum of MCAPUU, the band at $1,256\text{ cm}^{-1}$ is assigned to the stretch vibration of $\text{C}-\text{N}$ bond. In addition, the absorption band at $1,675\text{ cm}^{-1}$ is attributed to the carbonyl of urethane bond, showing that the MCAPUU contained the $-\text{NHCOO}-$ group. It also shows that the absorption band at $1,658\text{ cm}^{-1}$ is assigned to the carbonyl of urea bond, indicating the existence of $-\text{NHCONH}-$ groups. The disappearance of the peak at $2,273\text{ cm}^{-1}$, which corresponded to the $-\text{NCO}$ group, indicated that the $-\text{NCO}$ had reacted with $-\text{NH}_2$ completely.

Thermal, mechanical and physical properties of MCAPUU film

The film was prepared by casting onto a poly (tetrafluoroethylene) at $60\text{ }^\circ\text{C}$ for 48 h. Differential scanning calorimetry (DSC) and thermogravimetric analysis (TGA) were performed and the curves were shown in Supplementary information Figure S3. It can be seen that the glass transition temperature (T_g) of hard segment and the decomposition temperature (T_d) at 5 % mass loss of MCAPUU are 136 and $276\text{ }^\circ\text{C}$, respectively.

The mechanical properties such as tensile strength, elongation at break and hardness of MCAPUU film were measured and the results are 2.97 MPa , 967.61% and 65 , respectively.

The thermal conductivity, thermal diffusion coefficient, density and specific heat capacity of MCAPUU film were obtained from a thermal conductivity detector

(TC3010, Xi'an Xiayi Electronic Technology Co., Ltd, Xi'an, China) at room temperature and the results are 0.17374 W/(m K), 1.33×10^{-8} m²/s, 1,356 kg/m³ and 5.826 kJ/(kg K), respectively.

Thermo-optical coefficient, dispersion property and transmission loss of MCAPUU film

Thermo-optic coefficient (dn/dT) is the variation of refractive index depending on the temperature and is the main factor to affect the driver power and response speed of the optical switch [24, 25]. In the experiment, the prepared MCAPUU solution, which was filtered through a syringe with a 0.45 μm Teflon filter before it was applied, was spin-coated onto the hypotenuse face of a prism and dried in vacuum overnight at room temperature to evaporate traces of the solvents. Then, a laser beam ($\lambda = 532, 650$ or 850 nm) passed through a polarizer, then reached the interface between the prism and the gold film with an appropriate angle. The reflected light was detected by a photodiode and averaged to reduce the noise. The prism–waveguide coupling system and detector were mounted on a high-precision $\theta/2\theta$ computer-controlled goniometer and a series of dips in reflectivity due to resonant transfer of energy into guide modes were generated on a computer screen and saved in a data file. The various synchronization angles of the attenuated total reflection (ATR) spectra at different temperature and laser beam ($\lambda = 532, 650$ or 850 nm) were measured. The refractive indices of TE (transversal electric) polarization at different temperature and different single wavelength (532, 650 or 850 nm) were calculated and listed in Table 1. From the Table 1, the refractive index of MCAPUU gradually decreased as the temperature increases at different single wavelength. The thermo-optic coefficients of MCAPUU film are -4.5429×10^{-4} $^{\circ}\text{C}^{-1}$ (532 nm), -5.7943×10^{-4} $^{\circ}\text{C}^{-1}$ (650 nm) and -6.6057×10^{-4} $^{\circ}\text{C}^{-1}$ (850 nm), respectively.

The dispersion relation between refractive index and wavelength is expressed by Sellmeyer dispersion equation:

$$n = A + \frac{B}{\lambda^2} + \frac{C}{\lambda^4} \quad (6)$$

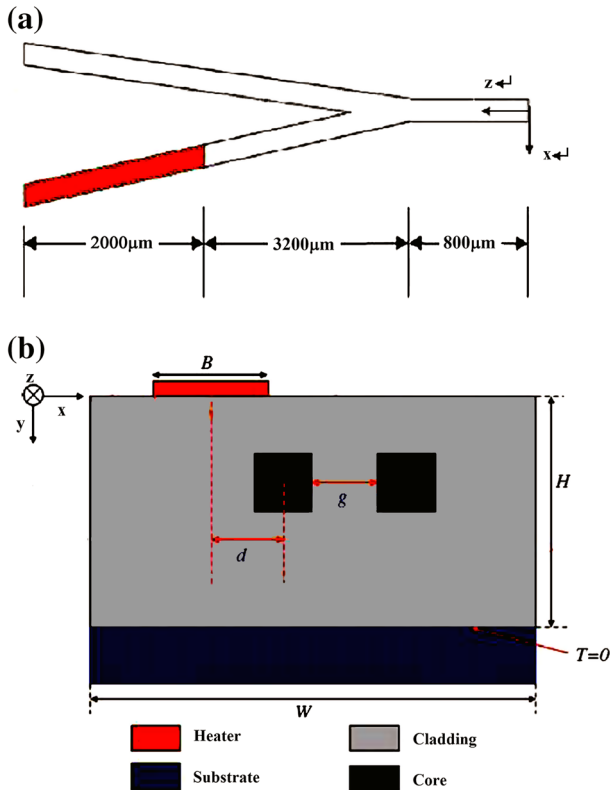
where λ is the incident laser wavelength (vacuum), and A, B and C are the coefficients of Sellmeyer dispersion equation. The coefficients A, B and C of MCAPUU film at different temperature are shown in Table 2.

Table 1 The refractive index of MCAPUU film

Wavelength (nm)	T ($^{\circ}\text{C}$)						dn/dT ($\times 10^{-4}$ $^{\circ}\text{C}^{-1}$)
	15	20	25	30	35	40	
532	1.4739	1.4695	1.4673	1.4650	1.4641	1.4617	-4.5429
650	1.4672	1.4660	1.4618	1.4585	1.4563	1.4534	-5.7943
850	1.4644	1.4633	1.4592	1.4552	1.4521	1.4488	-6.6057

Table 2 The Sellmeyer coefficient of MCAUU film

Coefficient	T (°C)					
	15	20	25	30	35	40
A	1.4649	1.4599	1.4587	1.4539	1.4499	1.4526
B (nm) ² ($\times 10^3$)	-2.2037	-2.3051	-0.9968	-0.5077	-0.0611	-4.3184
C (nm) ⁴ ($\times 10^9$)	1.3471	0.1179	0.9631	1.0306	1.1204	1.9380

**Fig. 1** The sketch (a) and cross section (b) structures of a polymeric thermo-optic DOS

The charge coupled device (CCD) digital imaging devices are used to measure the scattered relative light intensity distribution of optical polymer. The measured curve of transmission loss for MCAUU film is shown in Supplementary information Figure S4. The transmission loss value is 0.130 dB/cm.

Design and simulation of Y-branch thermo-optic switch

In this work, the sketch (a) and cross section (b) structures of a polymeric thermo-optic digital optical switch (Y-branch) based on silicon substrate by etching out the

air channel between branches were designed and shown in Fig. 1. The MCAPUU thin-film waveguide was determined to be buried square waveguide (BSC) with a $3 \times 3 \mu\text{m}^2$ cross section. The BSC waveguides have the advantage of good fiber-to-waveguide coupling and little polarization dependency compared with the rectangular waveguide. When the heater is turned on, the refractive index under the heater decreases due to the thermo-optic characteristics of the polymer material.

The upper cladding thickness was determined to be $5 \mu\text{m}$ to avoid mode attenuation to the heater. The refractive indices of core and cladding are 1.4608 and 1.4508 ($1,550 \text{ nm}$), respectively. The thermo-optic coefficient of MCAPUU film at $1,550 \text{ nm}$ is $-5.8700 \times 10^{-4} \text{ }^\circ\text{C}^{-1}$ according to Table 2. The other used parameters for the MCAPUU film such as the thermal conductivity, density and specific heat capacity are given in “[Thermal, mechanical and physical properties of MCAPUU film](#)”. With these parameters and the branching angle of 0.143° , the thermo-optic switch was analyzed using finite difference beam propagation method (FD-BPM) by introducing constant refractive index difference (Δn) between branches along propagation distance which led to the difference in effective refractive index (ΔN_{eff}).

The field distribution at the output waveguides with heating of MCAPUU is shown in Supplementary information Figure S5. It can be seen that the thermo-optic effect could influence the optical field. The optical power of the output terminal was calculated when two branches had different refractive indices. The output power dependence on Δn is shown in Fig. 2. From the Fig. 2, the thermo-optic switches all are turned off when the Δn is 5.5×10^{-4} .

The distribution of optical field at $\Delta n = 5.5 \times 10^{-4}$, distribution of temperature at $Z = 4,000 \mu\text{m}$ and isotherm of temperature field are shown in Figs. 3, 4 and Supplementary information Figure S6, respectively. According to the thermo-optic coefficient, when the heat rates of the heating electrodes is $9.2 \times 10^4 \text{ W/m}^2$, the

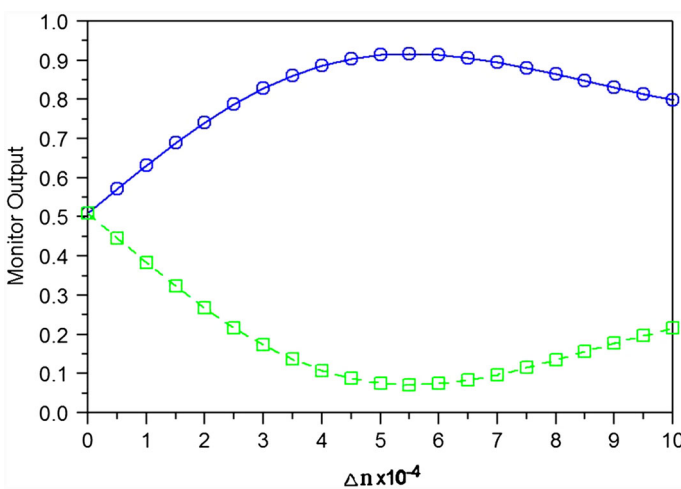


Fig. 2 The relationship between output power and Δn of MCAPUU

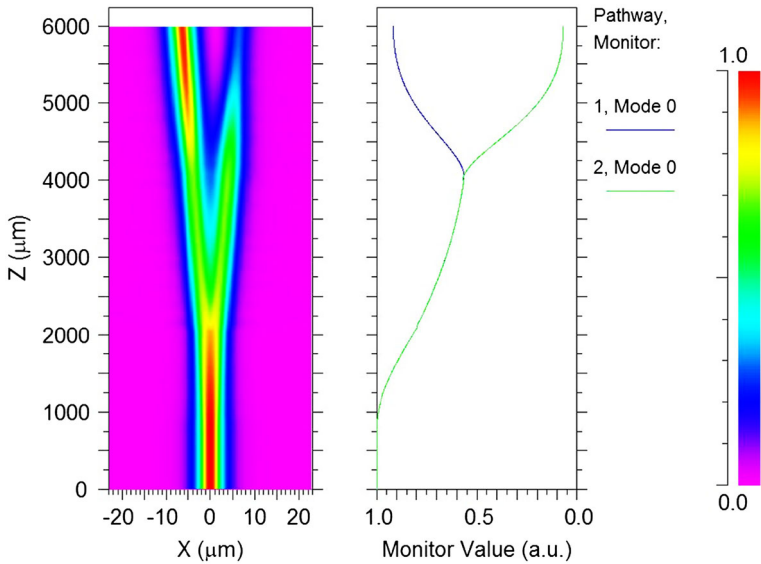


Fig. 3 The distribution of optical field at $\Delta n = 5.5 \times 10^{-4}$ of MCAPUU

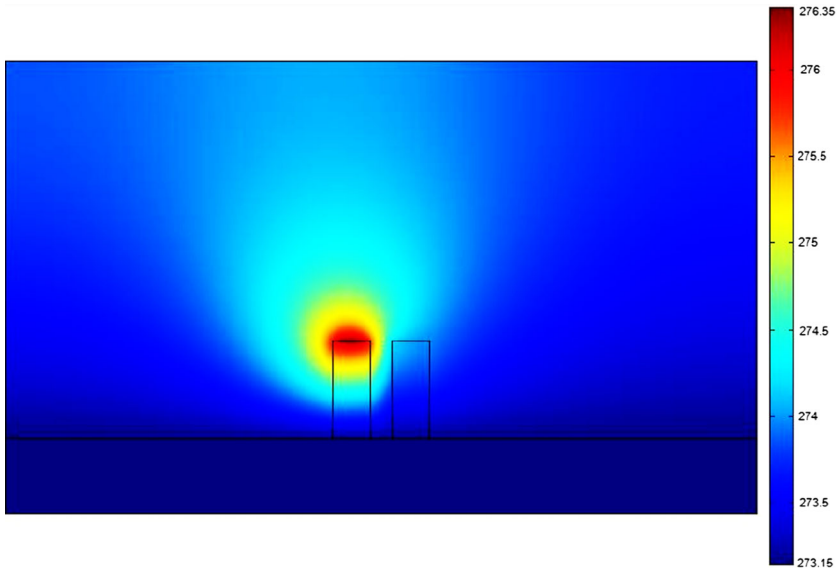


Fig. 4 The distribution of temperature field at $Z = 4,000 \mu\text{m}$ of MCAPUU

temperature difference of the sandwich layer of MCAPUU in the two branches is $0.77 \text{ }^\circ\text{C}$ and could meet the requirements. The power consumption of thermo-optic switch could be only 0.74 mW . The simulated switching behaviors in time (under the electrode heating) were also performed and are shown in Supplementary

information Figure S7. It can be seen that the stable temperature is 274.49 K and a 12.0-ms switching time can be achieved with the present design. This is a significant improvement in reducing the power consumption compared with those of the normal Y-branch polymer thermo-optic switch. This is mainly because the combination of a large thermo-optic (TO) coefficient with low thermal conductivity results in low electric switching power at ms-response time.

Design and simulation of Mach–Zehnder interferometer (MZI) thermo-optic switch

Mach–Zehnder interferometer (MZI) thermo-optic switch with two rib waveguides, dual driving electrodes and two critical 3-dB couplers based on thermo-optic effect of prepared MCAPUU was designed and shown in Fig. 5. The length of power divider, interference arm and arc are 416, 5,000 and 2,000 μm , respectively. The total length is 15,200 μm . The distance of the input port is 20 μm (center distance).

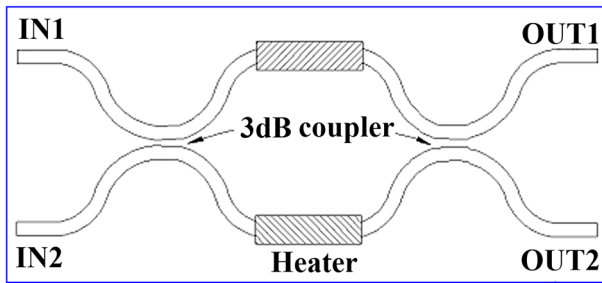


Fig. 5 Structural schematic of Mach–Zehnder interferometer (MZI) thermo-optic switch

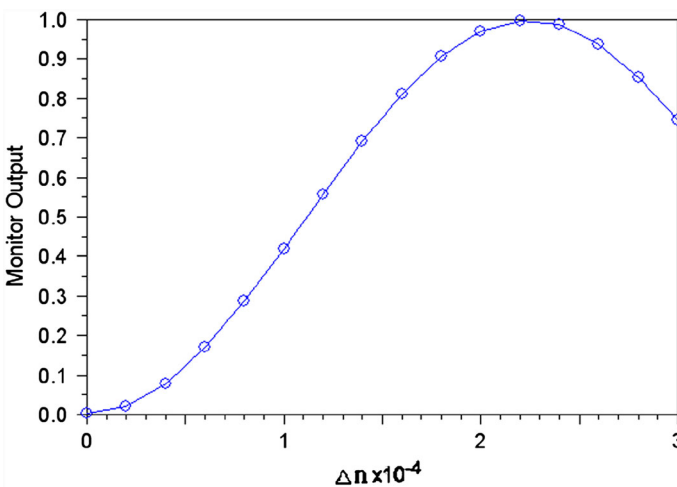


Fig. 6 The relationship between output power and Δn of MCAPUU

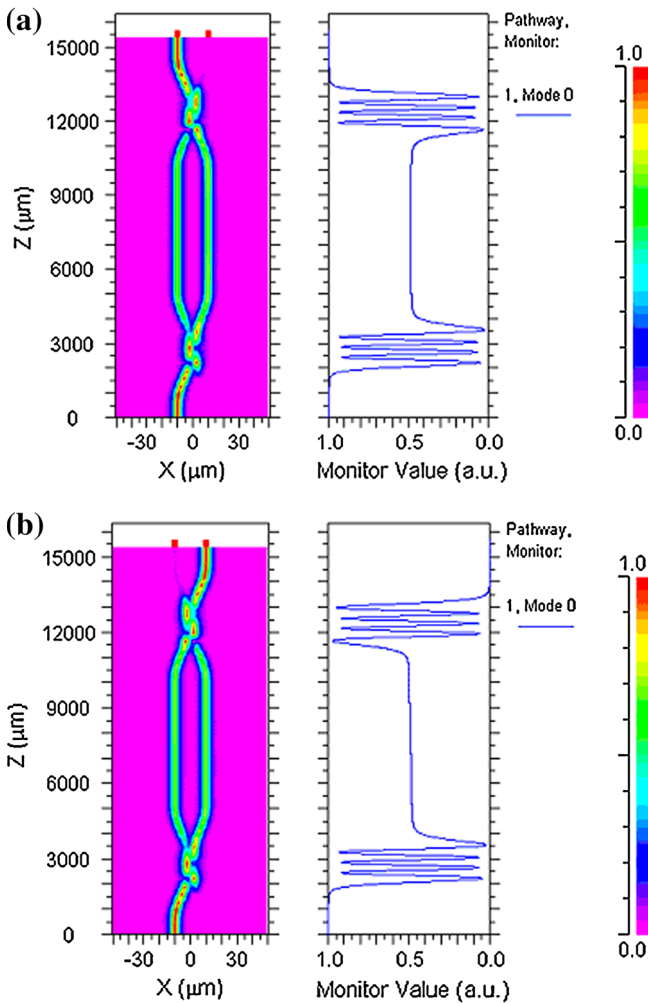


Fig. 7 The distribution of optical field of **a** turned on status and **b** turned off status

The distance of the narrowest point is $4\ \mu\text{m}$. The other parameters are the same as above.

The optical power of the output terminal was calculated when two arms had different refractive indices. The output power dependence on Δn is shown in Fig. 6. From Fig. 6, the thermo-optic switches all are turned off when the Δn was 2.2×10^{-4} . The distribution of optical field of MCAPUU when the switch is turned on or off and distribution of temperature field of steady state are shown in Figs. 7 and 8, respectively. According to the thermo-optic coefficient, when the heat rate of the heating electrodes is $5.0 \times 10^4\ \text{W/m}^2$, the temperature difference of the sandwich layer of MCAPUU in the two branches is $0.4748\ ^\circ\text{C}$. The response rising and falling times of the switches (under the electrode heating) were also performed

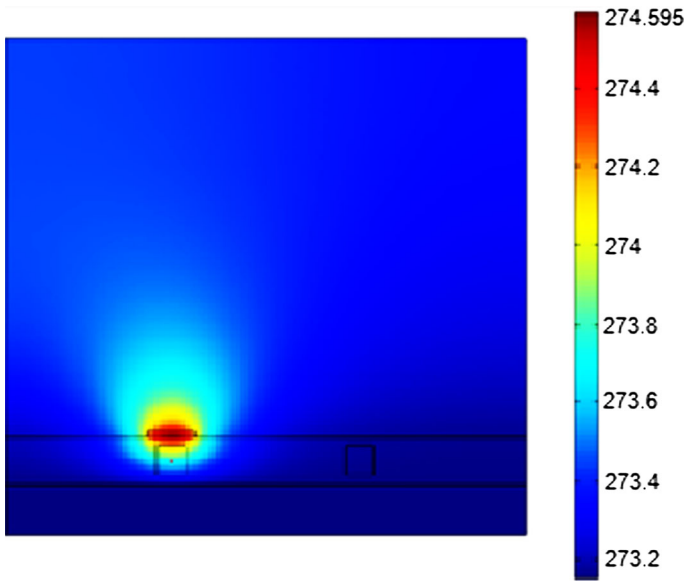


Fig. 8 The distribution of temperature field of steady state

and are shown in Supplementary information Figure S8. It can be seen that the rising (t_{rise}) and falling (t_{fall}) times are about 1.8 ms.

Conclusion

A novel main-chain azo polyurethane-urea (MCAPUU) was successfully prepared and the chemical structure was characterized by the FT-IR and UV–Visible spectroscopy. The glass transition temperature (T_g) and the decomposition temperature (T_d) at 5 % mass loss of MCAPUU were 136 and 276 °C, respectively. The mechanical properties such as tensile strength, elongation at break and hardness of MCAPUU film were measured and the results were 2.97 MPa, 967.61 % and 65, respectively. The thermal conductivity, thermal diffusion coefficient, density and specific heat capacity of MCAPUU film were 0.17374 W/(mK), 1.33×10^{-8} m²/s, 1,356 kg/m³ and 5.826 kJ/(kg K), respectively. The refractive index was measured at different temperatures and wavelengths by ATR technique. The thermo-optic coefficients (dn/dT) of MCAPUU were -4.5429×10^{-4} °C⁻¹ (532 nm), -5.7943×10^{-4} °C⁻¹ (650 nm) and -6.6057×10^{-4} °C⁻¹ (850 nm), respectively. The results showed that the MCAPUU film has large thermo-optic (TO) coefficients and low thermal conductivity. The transmission loss of MCAPUU film was obtained using CCD digital imaging devices and the value 0.130 dB/cm. A Y-branched switch was simulated, and the results showed that the power consumption of the thermo-optic switch could be only 0.74 mW, and the response time of the switch could reach about 12 ms. The MZI switch was simulated and the

result showed that the response time of the MZI switch is about 1.8 ms. The results indicated that the prepared MCAUU has high potential for the applications of the Y-branch digital optical switch (DOS), MZI thermo-optic switch and other optical modulators.

Acknowledgments This project was supported by the Agricultural Independent Innovation of Jiangsu Province (CX(11)2032), China Postdoctoral Science Foundation (2011M500865), Jiangsu Planned Projects for Postdoctoral Research Funds (1002033C) and the Innovation Program for Graduate Education of Jiangsu Province (CXZZ12_0696).

References

1. Wang PF, Semenova Y, Zheng J, Wu Q, Hatta AM, Farrell G (2011) Proposal for a simple integrated optical ion-exchange waveguide polarizer with a liquid crystal overlay. *Opt Commun* 284:979–984
2. Fernandez R, Ramos JA, Esposito L, Tercjak A, Mondrago I (2011) Reversible optical storage properties of nanostructured epoxy-based thermosets modified with azobenzene units. *Macromolecules* 44:9738–9746
3. Hvilsted S, Sanchez C, Alcalá R (2009) The volume holographic optical storage potential in azobenzene containing polymers. *J Mater Chem* 19:6641–6648
4. Liu JH, Qiu FX, Cao GR, Guan YJ, Shen Q, Yang DY, Guo Q (2011) Chiral azo polyurethane(urea): preparation, optical properties and low power consumption polymeric thermo-optic switch. *J Polym Sci B* 49:939–948
5. Beharry AA, Sadovski O, Woolley GA (2011) Azobenzene photoswitching without ultraviolet light. *J Am Chem Soc* 133:19684–19687
6. Qiu FX, Da ZL, Yang DY, Cao GR, Li PP (2008) The synthesis and electro-optic properties of polyimide/silica hybrids containing the benzothiazole chromophore. *Dyes Pigments* 77:564–569
7. Zhang XQ, Wang CS, Lu XM, Zeng Y (2011) Nonlinear optical response of liquid crystalline azo-dendrimer in picosecond and CW regimes. *J Appl Polym Sci* 120:3065–3070
8. Alam MZ, Ohmachi T, Ogata T, Nonaka T, Kurihara S (2006) Surface relief gratings on azo polymer films through reversible photoisomerization by the irradiation of a monochromatic light. *J Appl Polym Sci* 102:3123–3126
9. Mysliwiec J, Miniewicz A, Nespurek S, Studenovský M, Sedlakova Z (2007) Efficient holographic recording in novel azo-containing polymer. *Opt Mater* 29:1756–1762
10. Cipparrone G, Pagliusi P, Provenzano C, Shibaev VP (2010) Polarization holographic recording in amorphous polymer with photoinduced linear and circular birefringence. *J Phys Chem* 114:8900–8904
11. Zhang YY, Cheng ZP, Chen XR, Zhang W, Wu JH, Zhu J, Zhu XL (2007) Synthesis and photo-responsive behaviors of well-defined azobenzene-containing polymers via RAFT polymerization. *Macromolecules* 40:4809–4817
12. Zhao Y, Qi B, Tong X, Zhao Y (2008) Synthesis of double side-chain liquid crystalline block copolymers using RAFT polymerization and the orientational cooperative effect. *Macromolecules* 41:3823–3831
13. Wu YL, Natansohn A, Rochon P (2004) Photoinduced birefringence and surface relief gratings in polyurethane elastomers with azobenzene chromophore in the hard segment. *Macromolecules* 37:6090–6095
14. Xu ZS, Drnoyan V, Natansohn A, Rochon P (2000) Novel polyesters with amino-sulfone azobenzene chromophores in the main chain. *J Polym Sci A* 38:2245–2253
15. Ehsan AA, Shaari S, Abd Rahman MK (2011) Acrylic and metal based Y-branch plastic optical fiber splitter with optical NOA63 polymer waveguide taper region. *Opt Rev* 18:80–85
16. Ho WF, Chan WY, Uddin MA, Chan HP (2008) Reliability of epoxy-based polymer optical waveguide devices under high temperature. *J Optoelectron Adv Mater* 10:434–441
17. Kim KT, Han BJ, Kim MK, Kim YH, Lee BH, Cho KJ, Kim JW, Lee CH, Lee J (2011) 4×4 Plastic optical fiber star coupler incorporated with a common polymer waveguide optical power distribution region. *Fiber Integr Opt* 30:265–277

18. Kim S, Cha D, Pei QB, Geary K (2010) Polymer optical waveguide switch using thermo-optic total-internal-reflection and strain-effect. *IEEE Photonic Technol Lett* 22:197–199
19. Qiu FX, Cao ZJ, Cao GR, Guan YJ, Shen Q, Wang Q, Yang DY (2012) Preparation, optical properties and 1×2 polymeric thermo-optic switch of polyurethane-urea. *Mater Chem Phys* 135:518–523
20. Al-Hetar AM, Mohammad A, Supa'at AM, Shamsan ZA (2011) MMI-MZI polymer thermo-optic switch with a high refractive index contrast. *J Lightwave Technol* 29:171–178
21. Yulianti I, Supa'at ASM, Idrus SM, Al-Hetar AM (2010) Cosine bend-linear waveguide digital optical switch with parabolic heater. *Opt Laser Technol* 42:180–185
22. Cao ZJ, Yan YF, Meng J, Jin L, Zhang DM (2012) Low power consumption thermo-optic switch based on DR1/PMMA. *Microwave Opt Technol Lett* 54:2163–2165
23. Lee MH, Min YH, Park S, Ju JJ, Do JY, Park SK (2002) Fully packaged polymeric four arrayed 2×2 digital optical switch. *IEEE Photonic Technol Lett* 14:615–617
24. Liu JH, Qiu FX, Cao GR, Shen Q, Cao ZJ, Yang DY (2011) Preparation, thermo-optic property and transmission loss of chiral azobenzene polyurethane. *J Appl Polym Sci* 121:2567–2572
25. Qiu FX, Zhang W, Liu JH, Yang DY (2010) Optically active polyurethane containing asymmetric center: preparation, characterization and thermo-optic properties. *Polym Plast Technol Eng* 49:1521–1526